Pakistan Academy of Sciences

Research Article

CFD Analysis to Study the Effect of Geometry in Flow Behavior of Wing Structure with Additional Riblets

**Muhammad Zia Ullah Khan[1], Rumeel A. Bhutta[1], Tahir Asif[2,*],
Muhammad Farooq[2], and Adnan Qamar[2]**

[1]Mechanical Engineering Department,
COMSATS Institute of Information Technology, Sahiwal, Pakistan
[2]Mechanical Engineering Department,
University of Engineering & Technology, Lahore, Pakistan

Abstract: Drag reduction have always been the most important area of interest for a decade with many advancement in it, there has been continuous research on the flow behavior of wing with different geometric combination. Previous studies suggest that Riblets are 7% effective given that they are made with correct sizing. According to test conducted shows the near same result of drag reduction up to 5%. In the present research CFD techniques were used to analyze the flow pattern, where geometry was changed in addition to Riblets named as add-ins. Pressure effect and corresponding velocity dynamics were studied. Each reformed airfoil was analyzed using CFD techniques. A structured grid mesh was used. Governing equation were identified to model exact behavior and numerical computation was performed using FEA software. Simple algorithm and second order upwind scheme for pressure discretization, second order upwind scheme for momentum and energy was used. Changing geometric shape shifts pressure regions and more control is obtained on lift. Value extraction zone selected is outer cross-sectional area in close approximation to wing profile using commercially available computational package. ΔP at point 0.05 for design 1,2 and 3 at $0°$ is 5400 Pa, 7000 Pa and 100 Pa, at $15°$ on far location is 26000 Pa, 4000 Pa and 8000 Pa where on close location is 35000 Pa, 18000 Pa and 5000 Pa which shows good feasibility for first two designs. Design 1 and 4 ΔP at 0.05 is 500 Pa and 4000 Pa. Singular geometric alteration yields better result than plural, any modification to rear section does not affect the flow separation. By doing these amendments on desired points can increasing fuel economy rate for jets and commercial air planes.

Keywords: Addition of riblets, computational modeling, velocity profile, wing geometry analysis

Nomenclature

|			
P	Density	τ_{ij}	Stress tensor
t	Time	u_i	Orthogonal velocities
V_x, V_y, V_z	Velocities	μ	Dynamic viscosity
P	Pressure	μ_e	Effective viscosity
R	General gas constant	λ	Second coefficient of viscosity
T	Temperature	μm	Micrometre

1. INTRODUCTION

Riblets are small patches on the surface of wing that makes a turbulent flow unidirectional. Riblet and their ratio effectives depends on protrusion size [1, 2]. Micro protrusions have significant effect in friction and viscous drag reduction, it is worth studying that how the flow behavior change if these small protrusion are added to the down side of the wing. V-grooved shaped riblet proved to most efficient [3, 4], study of NACA 0012 showed 4.3%

drag reduction [5] while in [6] drag reduction of 4% to 7% on flat surfaces. Sand paper strip was used to give micro structured effect at the leading edge of airfoil NACA 0012 showing adverse effect on velocity [7] like other studies consideration was given to the upper section of airfoil, where amalgamation of riblets and gurney flaps gives no positive result [4, 8]. Since riblets are considered as an auxiliary change to the structure to enhance flow behavior, its transition from laminar to turbulent

increasing overall efficiency of airfoil, and any structure change in airfoil geometry is ranked on how it effects these variables. The variation in local velocity profile for hairy surface is similar to the surface with riblets [9] as velocity profile passages away from surface reducing skin friction. Numerical drag reductions were not verified by the experimental data [10]. Same hairy like effect was tested based on owl wing surface by using two velvet like surfaces concluded that separation bubble does not depend on the angle of attack and enhances the aerodynamic performance of wing [8]. This phenomena helps birds to fly with best efficiency but cannot be imitative for practical applications. Rice and butter wing effect introduced by Bixler and Bhushan, anisotropic flow leading to low drag was found due to aligned shingle-like scales in butterfly wings and sinusoidal grooves in rice leaf [11]. Same results were found when microstructure inspired by shark-skin is tested [12].

Ribbed coating of polymeric film bonded to the upper and lower surface of wing, lateral and vertical aerodynamics are effected by coating also it proved to have negligible effect on longitudinal aerodynamic moments [13]. Biologically inspired microstructures where are useful but on other hand hard to implement practically on large scale. Experiment by [14] on NACA 0012 airfoil by the use of Miro-Riblet Film (MRF) showed that it decreases the overall height of vortices increasing the drag force on wing. Riblets were found to be as good passive controller in reduction of secondary flow where observed setup had riblets placed in front of wing [15]. Solitary use of riblets becomes ineffective once dirt and weather parameters are introduced into the practical equation [16].

Up to authors' knowledge recent literature in this area focuses on effect of riblets in upper section of airfoil. In this very research change in airfoil geometry in lower section of wing termed as add-in, is studied, paralleled with normal structure, structure with riblet and with combination of riblet and add-in.Simple yet effective technique of CFD is used to study such geometric changes. Airfoil used for this is of Boeing 737 MIDSPAN cross sectional area. All these simulation are scaled down to one fifty of their original model as most of the parameters estimating the pressure gradient,
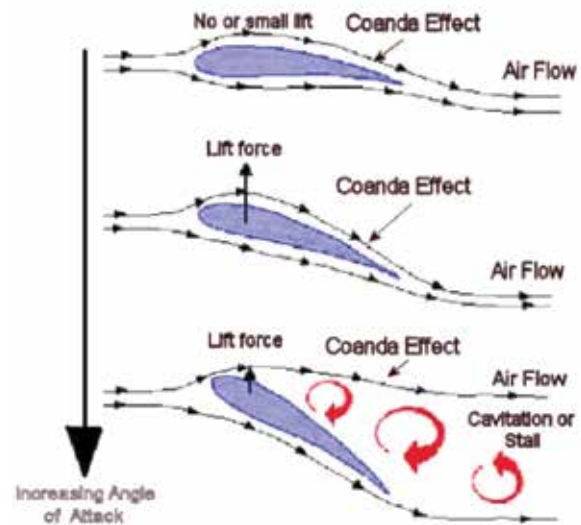
Fig. 1. Flow behavior and properties associated with it [22].

velocity and turbulence association are all being dimensionless and would not affect the overall result aiding to characterize and identify pressure with change in design, add in contribution to overall behavior, best optimal location for add-in.

Different shapes invokes different behaviors in Riblets [17], Fig. 1 rotating wing about an axis perpendicular to direction of flow and considering rear edge to be origin, as angle of rotation increases more frontal area comes in contact with air which generates vortices to the upper side of wing and if angle escalates wing will reach a condition known as stall where it no longer generates lift and same case can be considered with add-ins.

2. METHODS

2.1. Theoretical Formulation

Laws of conservation of momentum, mass and energy are used to explain the fluid flow behaviors [18]. These are then solved in term of differential equations. Assumptions are to be made in order to solve such equations as laminar flow, one phase existence. Keeping these assumptions the governing equations are:

$$\frac{\partial \rho}{\partial t} = \frac{\partial(\rho V_x)}{\partial x} + \frac{\partial(\rho V_y)}{\partial y} + \frac{\partial(\rho V_z)}{\partial z} = 0 \qquad \text{(i)}$$

Equation (i) is continuity equation which can be deduced form law of conservation of mass [19]. For

simulation above equation is solved by replacing the rate of change of density (ρ) with that of rate of change of pressure (P) according to which density changes with pressure. Equation (ii) specifies this as,

$$\frac{\partial \rho}{\partial t} = \frac{\partial \rho}{\partial P} \frac{\partial P}{\partial t} \qquad (ii)$$

Where P is the pressure. Since air is assumed to be ideal gas, then the evaluation of the derivation of density can be done from the equation of state by equation (iii) as,

$$\rho = \frac{P}{RT} \Rightarrow \frac{\partial \rho}{\partial t} = \frac{1}{RT} \qquad (iii)$$

R and T are gas constant. Air being a Newtonian fluid so the relationship between rate of deformation of fluid and stress can be described by equation (iv) as:

$$\tau_{ij} = -P\delta_{ij} + \mu \left(\frac{\partial u_i}{\partial x_j} + \frac{\partial u_j}{\partial x_i} \right) + \delta_{ij} \lambda \frac{\partial u_i}{\partial x_i} \qquad (iv)$$

Where τ_{ij} is stress tensor, u_i are orthogonal velocities μ is dynamic viscosity and λ is the second coefficient of viscosity. This relationship is simplified after solving and neglecting some term for compressible fluid for x, y and z component respectively we get three equations,

$$\frac{\partial \rho V_x}{\partial t} + \frac{\partial(\rho V_x V_x)}{\partial x} + \frac{\partial(\rho V_y V_x)}{\partial y} + \frac{\partial(\rho V_z V_x)}{\partial z}$$

$$= \rho g_x - \frac{\partial \rho}{\partial x} + R_x + T_x + \frac{\partial}{\partial x}\left(\mu_e \frac{\partial V_x}{\partial x} \right)$$

$$+ \frac{\partial}{\partial y}\left(\mu_e \frac{\partial V_x}{\partial y} \right) + \frac{\partial}{\partial z}\left(\mu_e \frac{\partial V_x}{\partial z} \right) \qquad (v)$$

$$\frac{\partial \rho V_y}{\partial t} + \frac{\partial(\rho V_y V_x)}{\partial x} + \frac{\partial(\rho V_y V_y)}{\partial y} + \frac{\partial(\rho V_y V_z)}{\partial z}$$

$$= \rho g_y - \frac{\partial \rho}{\partial y} + R_y + T_y + \frac{\partial}{\partial x}\left(\mu_e \frac{\partial V_y}{\partial x} \right)$$

$$+ \frac{\partial}{\partial y}\left(\mu_e \frac{\partial V_y}{\partial y} \right) + \frac{\partial}{\partial z}\left(\mu_e \frac{\partial V_y}{\partial z} \right) \qquad (vi)$$

$$\frac{\partial \rho V_z}{\partial t} + \frac{\partial(\rho V_z V_x)}{\partial x} + \frac{\partial(\rho V_z V_y)}{\partial y} + \frac{\partial(\rho V_z V_z)}{\partial z}$$

$$= \rho g_z - \frac{\partial \rho}{\partial z} + R_z + T_z + \frac{\partial}{\partial x}\left(\mu_e \frac{\partial V_z}{\partial x} \right)$$

$$+ \frac{\partial}{\partial y}\left(\mu_e \frac{\partial V_z}{\partial y} \right) + \frac{\partial}{\partial z}\left(\mu_e \frac{\partial V_z}{\partial z} \right) \qquad (vii)$$

Where μ_e is the effective viscosity; in the instant case effective viscosity is the dynamic viscosity.

Energy equation solution is not required as flow behavior is studied. All these equation are used by FEA package to stimulate flow. All the terms for z distribution are neglected due to 2D analysis and other reason for this is that introducing another dimension to the analysis complicates the deduction of flow behavior which is not required.

2.2. Modeling Conditions

Fig. 2 shows the cross-section of the geometries with location of riblet and add-in on upper and lower portion of airfoil for all designs, used for the present analysis, and along with it is the mesh produced situation which consist of structural mesh of 77188 nodes and 38129elements around and on the plane. Domain fifteen times the airfoil form
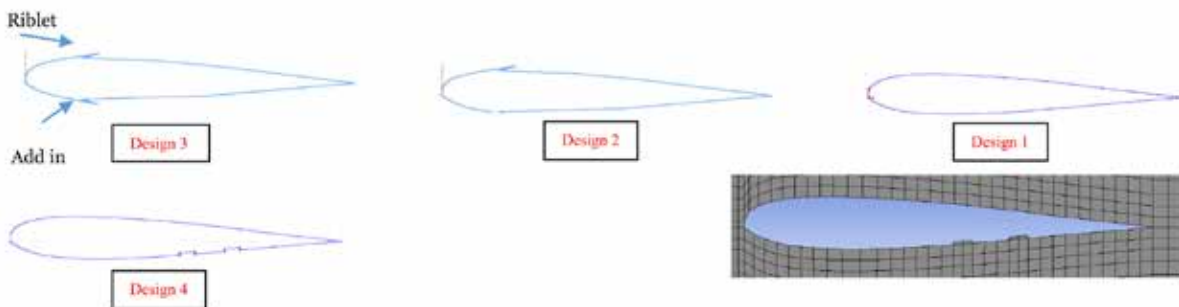

Fig. 2. Wing cross-sections showing different changes (Design 1-4).

origin to upper and lower Y axis limit, seven times to front and twenty five times to back, to capture proper flow on leaving regime. Inlet boundary condition of 330m/s, outlet is set to gauge pressure. No slip condition on outer walls of domain. These boundary conditions are being used one by one which change in shape and angle of attack.

2.3. Analysis Factor

Analysis was carried out with simple algorithm and second order upwind scheme for pressure discretization, second order upwind scheme for momentum and energy too. Neglecting atmospheric extreme weather conditions like snow or volcano eruption[16], using air as working fluid with its respective flow properties. Relaxation factors are taken to be default values of pressure 0.3, density 1, body forces 1, momentum 0.7 and turbulent kinetic energy 0.8. Convergence criterion set for 0.001 for continuity, x-momentum and y-momentum. Initial velocity is 330m/s. Boundary condition for pressure is zero gauge.

3. RESULTS AND DISCUSSION

Fig. 3-5, pressure and flow behavior with each profile is different as lift is a force generated by turning a moving fluid. Fig. 3, pressure dispersal around the airfoil is symmetric for 0°with change in angle from 0°to 15° variations starts to occur and force per unit area on the tip increases. Molecules close to surface have little or no motion due to skin friction drag and is same on upper and lower surface in case of 0° at 15° they stay attached to

lower surface but separation on molecular layer is observed on upper surface same as in [20], which shows parting from wing surface but molecules remain attached to upper flow boundary forming a smooth layer of flow followed by vortices region. Flow then stabilizes in regime after.   Fig. 4, alteration in wing profile on upper surface depicts no significance visual flow pattern modification for 0° in terms of ΔP when compared to not modified wing; however molecule separation from surface layer becomes substantial. Rotated to 15°, pressure uncertainty increases with small pressure bubble area formation at rear section acting as unit area force normal to surface downwards. Nevertheless this rotation shows positive results it also add more momentum to leaving air molecules making then to ring around one center forming big vortices on amended region. Formation point of these vortices is tip addition which no longer let the incoming layer over top surface to remain attach and as layer passes tip it starts to separate due to high velocity, where decrease in height of vortices is linked to high drag [14].

Fig. 5, same alteration in design on both surfaces shows symmetrical behavior of flow in terms of pressure and velocity, flow flinches to separate into small layers where particles of air on layer exhibiting coanda effect are collinear with the modified tip. This is the extreme point for flow disturbance and is symmetric to plane parallel to flow and passing through chord length. Comparison of Fig. 3-5, with no change flow behaves in its natural pattern, with change in one side natural pattern on that side is different where unchanged side of that very design
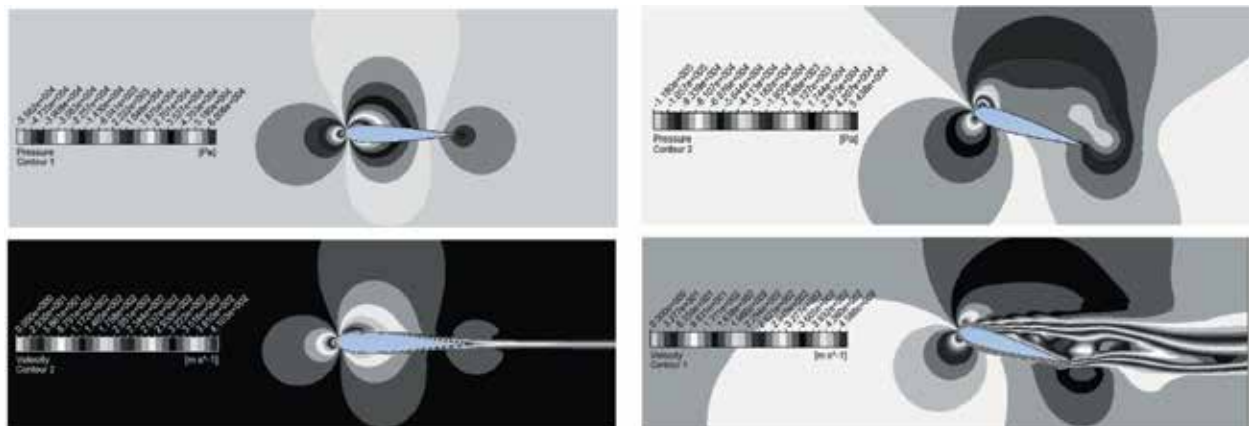

Fig. 3. Design 1 pressure (top) and velocity (below) Contour at 0^0 (left) and 15^0 (right) angle of attack.

still portrays the old natural behavior. Change on both sides pattern of side amended early simply gets mirrored with same results but now they are on the upper and lower side of the wing. From this study it is deducted that air foil that follows this mirror characteristics along chord length will produce no or little change when riblet and add-in are used combined. A better understanding of it can be observed by center of pressure (CoP) theory which is used to stabilize any object moving in fluid
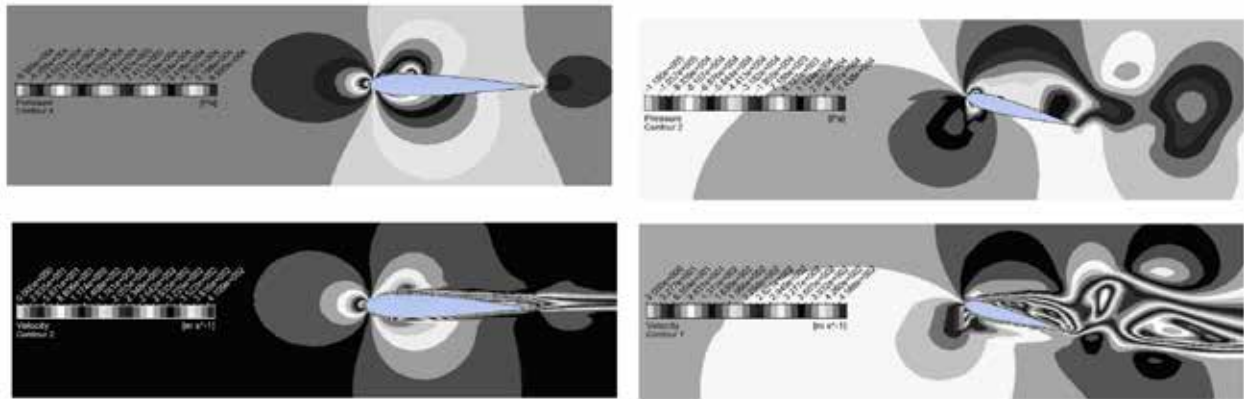

Fig. 4. Design 2 pressure (top) and velocity (below) Contour at 0^0 (left) and 15^0 (right) angle of attack.

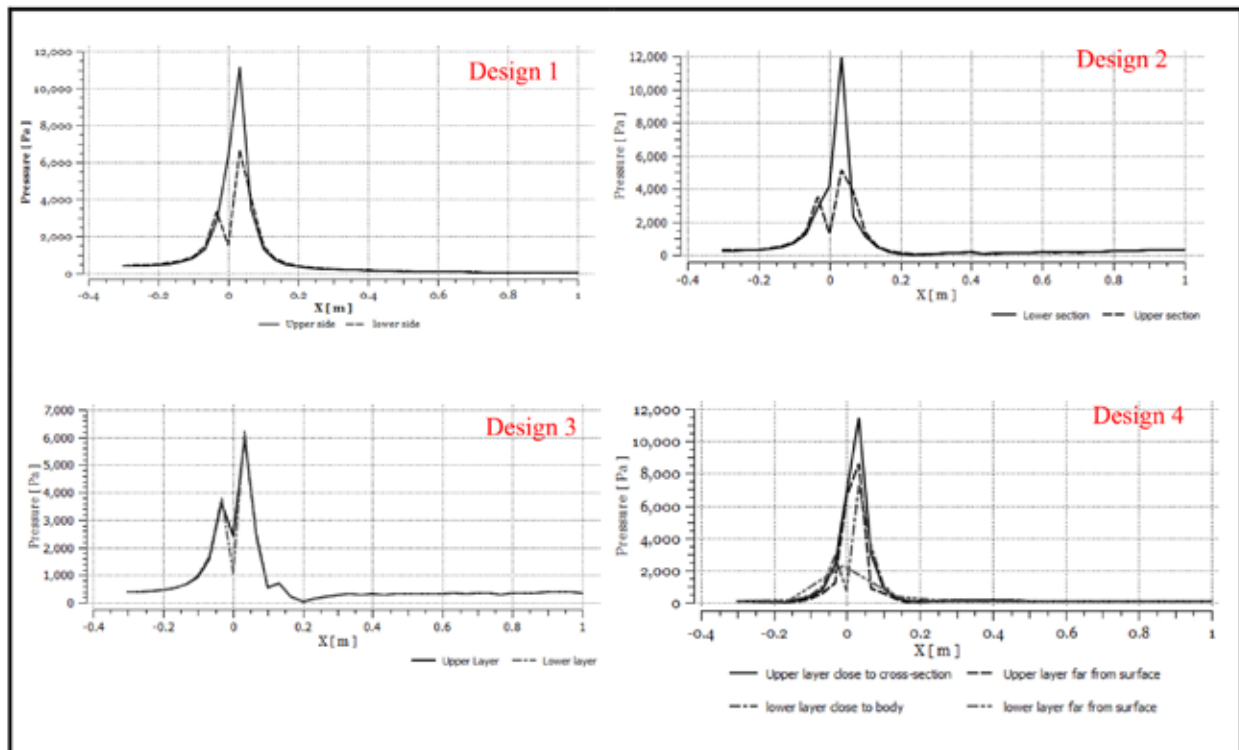**Fig. 5.** Design 3 pressure (top) and velocity (below) contour at 0^0.

Fig. 6. Pressure distribution around the airfoil at $0°$ attack angle.

as CoP changes which change in angle of attack so pattern of flow behavior will change according to it. Aerodynamic force is integration of pressure times surface area, lift and drag are the resolved components of this force, which acts through the center of pressure in flight. Increasing θ from 0° to 15° shifts CoP close to wing tip and thus producing more lift at the tip section. Fig. 3-5, CoP shift is same due to the fact that this protrusion size in practical is in μm so any kind of grove would not affect this transferal, as long as the air foil under study is same.

Fig. 6 shows that the pressure distribution on the nodes close and far on the both upper and lower side of the wings, on x-axis is the distance along which pressure varies. Graphs are generated for different geometric conditions for comparing the results and developing a proper conclusion. Legends show the discrimination between the upper and lower side flow on airfoil. Fig. 6design 1 upper side riblet causes more disturbance in the flow in term of pressure P and region where -0.2 < x < 0.3, is reverse flow which generates a little vacuum and is the cause of negative values.

3.1. Transverse Flow Assessment of Design 1, 2 and 3

Design 1 represents the tip type cross-section for the riblet on the upper side of the airfoil. Addition of riblet in shapes effects flow and pressure associated with it. Lower section defines the lower portion of wing and upper section defines upper layer close to wing bounding entities. Pressure shifts at upper section in region in between -0.2 to 0.2, having low values as compared to pressure at lower region. Variation in pressure raises the overall lift of wing.

Fig. 6 design 3 is graph between pressure *P* and distance *s*. It shows pressure dissemination in simple wing along x-direction, on regions enveloped by it at upper and lower portion on stated cross-section. Zero on x-axis represents tip of wing. Pressure increases as approaching air towards wing influences in region adjacent to wing tip. At tip sudden pressure drop followed by a peak pressure value. Gain in pressure is then reduces as flow enter the later region of wing from 0.05 m to 0.2 m, sliding over wing surface with high velocity. Both upper and lower layer have same curve paradigm.

After comparing designs in Fig. 6 graphs four designs at 0° angle of attack we find that the difference in pressure on the upper and lower side of airfoil is much greater for Design 1 while considering pressure difference at 0 point in graph. Whereas Design 2 pressure is at maximum of 12000 Pa higher than other designs.

Fig. 7 design 3 altered angle of attack to 15 degree with this change pressure elevates to tipple the amount as compared to 0 degree gave the same effect that of use of rough strip at leading edge [7]. Pressure divergence in upper and lower layer close to surface is in relation of low to high respectively. A spike in the negative direction in Fig. 7 design 1 shows a vacuum and reverse flow generation which is also visible on the contour visuals in Fig. 3. It can be seen that lower section of the wings have high pressure on the tip lower side of the wing as compared to upper side, indirect more lift as P_{lower} > P_{upper}.Fig. 3 design 4, upper close layer and far layer section pressure increases and to the point 0 to 0.05 and then decreases showing the same characteristics like design 1 in the upper section as the geometry is alike as far the lower section design 4 shifting in behavior for region far from cross section with an increase in pressure at the edge of the wing and having lower pressure around regions in close contact with the airfoil showing a 5% increase then design 1 at 0° attack angle.

Three peak values were observed which changes from design 1-3. First two designs have peak values at point 0 with a negative peak value followed by it. Pressure change for design 1 in Fig. 7 does not chart a smooth curve instead an abrupt change occurs along the flow direction generating some low pressure region below gauge pressure value. This phenomena is also observed with design 2 at 15° yet unlike design 1 curve change is not sudden but it first decreases then stabilizes for some distance between point 0 to 0.05 and then it descends again up to 0.1 and goes tends towards stabilizing again, this is the case in lower section of wing. In upper region pressure is in negative as soon as air particles comes in contact with wing tip pressure values decreases indication of vacuum in upper wing section and as the flow leaves the wing it stabilizes joining with the incoming flow from the lower side of the wing. Design 1 and 2 at 15°exhibit
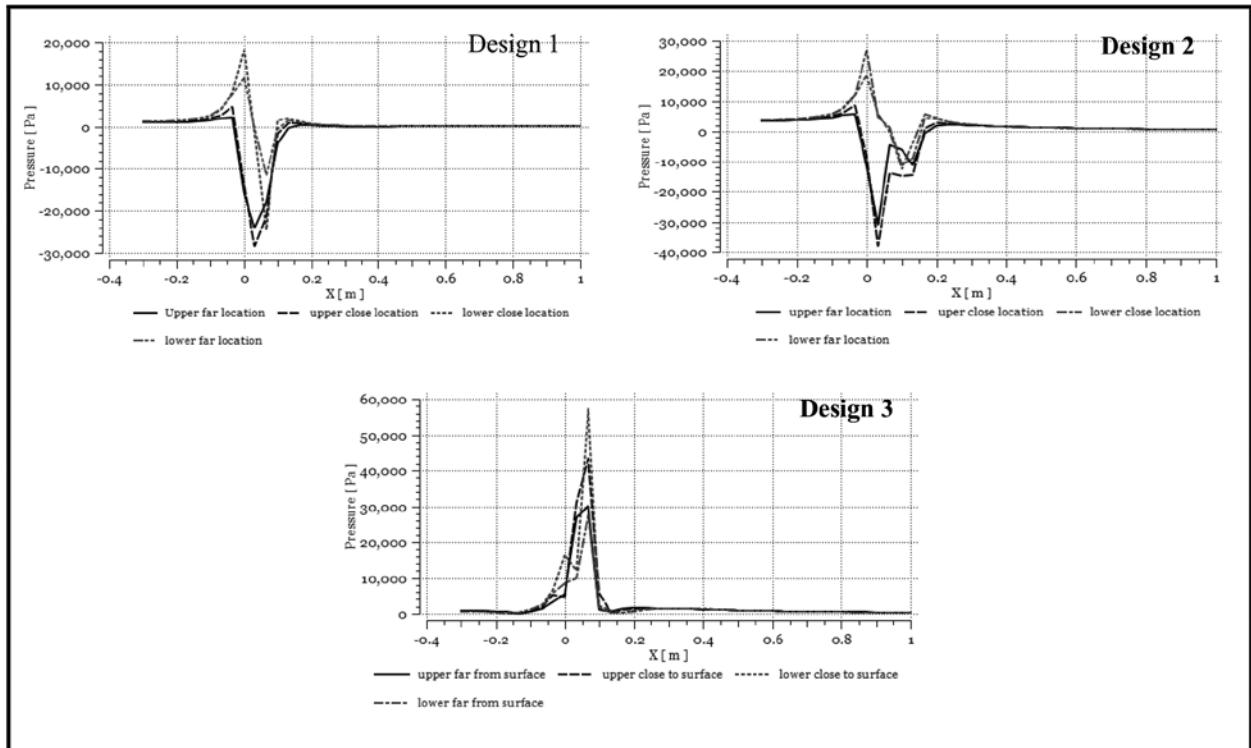
Fig. 7. Pressure distribution around the airfoil at 15° attack angle.

the same behavior but with different flow values. Design 3 in Fig. 7 have symmetric riblet and add-in, with a curve following the same behavior as of preceding graphs, to understand different behavior values taken for design were all positive and close comparison of all the layers showed that both upper layer had low value of 30000 Pa and 41000 Pa at point 0.05 while that of both lower layers had peak values reaching 54000 Pa at same point. Curve flow is abrupt same before graph.

Data values are extracted from the graph to evaluate each design behavior under specific location which is in table 1. Design 1-3 points 0, 0.05 and 0.1 along the flow direction are selected to assess pressure difference. Design 1-3 at point 0 gave pressure value of 4400 Pa , 2500 Pa and 1500 where at point 0.05 it gave 5400 Pa, 7000 Pa and 100 Pa and at 0.1 it had 100 Pa, 200 Pa and 0 Pa. At same point 0 all design have descending pressure values conversely at point 0.05 design 2 displayed an increase in pressure value this was due to alteration made to the foil. Derivative to point 0.1 with same analogy, on basis of this observation design 3 gives poor feasibility then design 1 and 2. With an increase in angle from 0° to 15° pressure

values elevated in surrounding regime far from wing surface, at point 0 gave pressure value of 27000 Pa, 32000 Pa and 4000 where at point 0.05 it gave 26000 Pa, 4000 Pa and 8000 Pa and at 0.1 it had 4000 Pa, 18000Pa and 200 Pa. Comparing those data values design 3 falls under poor feasibility due to low pressure difference in between locations. Regime far from wing surface gave low pressure values when compared to regime that is close to wing surface which are as at point 0 gave pressure value of 32000 Pa, 39000 Pa and 11000 where at point 0.05 it gave 35000 Pa, 18000 Pa and 5000 Pa and at 0.1 it had 2000 Pa, 6000Pa and 2000 Pa with poor feasibility for design 3 as it had truncated pressure at point 0 when equated with other designs at the same angle.

3.2. Transverse Flow Assessment of Design 1 and 4

Fig. 6, design 4 and design 1 make comparison of simple wing and wing with Add-in on lower side. For this comparison only upper layer close to cross-section and lower layer close to body is considered for Design 4 case to evaluate pressure difference at different points shown in Table 1 and were establish

Table 1. Comparison of airfoil at different angles along with practicability.

Geometry	Angle of attack	Pressure difference (Pa) at points			Feasibility
		(0 point)	(0.05 point)	(0.1 point)	
Design 1	0^0	4400	5400	100	Good
Design 2	0^0	2500	7000	200	Good
Design 3	0^0	1500	100	0	Poor
Pressure Difference on Surrounding Regime far from Wing Surface					
Design 1	$15°$	27000	26000	4000	Good
Design 2	$15°$	32000	4000	18000	Good
Design 3	$15°$	4000	8000	200	Poor
Pressure Difference on Surrounding Regime close to Wing Surface					
Design 1	$15°$	32000	35000	2000	Good
Design 2	$15°$	39000	18000	6000	Good
Design 3	$15°$	11000	5000	2000	Poor
Pressure Difference on Upper Layer close to Cross-section and Lower Layer close to Body					
Design 1	0^0	4300	500	100	Good
Design 4	0^0	6200	4000	100	Better then Design 1
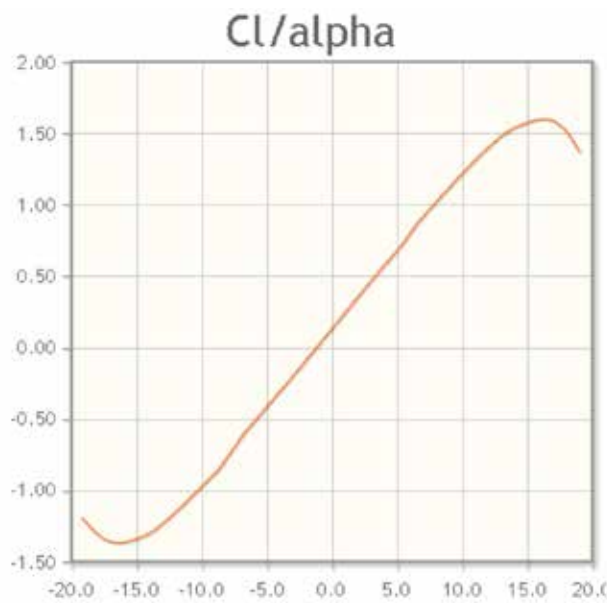
Fig. 8. Effect of angle of attack on lift co-efficient for Boeing 737 MIDSPAN Airfoil [23].

to be as at point 0 pressure value of 4300 Pa, 6200 Pa where at point 0.05 it gave 500 Pa, 4000 Pa and at 0.1 it had 100 Pa, 100 Pa. Pressure transformation in design 4 is smooth as it does not descends ascends with high gap between values unlikely than design 1 for which values were fluctuating with more gap in between them. Thus, proving design 4 at $0°$ to be

better than design 1.

Graph in Fig. 8 was generated using Xfoil online software to predict the effect of angle of attack on coefficient of lift. Maximum effective value of lift is in range of 15 degrees to 17 degrees. Increasing angle more than that decreases wing efficiency and tilted wing greater than 17 introduces frontal face drag parameter to the equation.

4. CONCLUSIONS

Four different alterations were done to airfoil in term of geometric point of view; each reformed airfoil was analyzed using CFD techniques. A structured grid mesh was used as it gives more stable result instead of hybrid or tetrahedral mesh topology. Flow behavior of air molecules were studied when subjected to different design changes along with attack angle change from $0°$ to $15°$ rotating wing about an axis perpendicular to direction of flow and considering rear edge to be origin. Coanda effect, stall condition, pressure distribution, air molecule flow behavior with first initial contact till final, wing design optimization and its effect of likelihood with-in the designs under study were premeditated. Each design was compared on the basis of pressure values covering the ari foil surrounding regime.

Changing conventional wing sections into new ones changes the flow pattern, but as for the sake of observation protrusion were kept to big size, which different changes Coanda effect and stall properties can be controlled and Riblets along with add-in have proven to be valuable to study such cases. Concept of CAM for riblet manufacturing which can be instigated to the add-in segment.

It is concluded that, theoretically add-in was a good approach in seeking better aerodynamic results but practically they could be of problem in extreme weather conditions like snow or volcano eruption where ash or small particles can get stuck in to these small protrusions. which is rare event like bird strike and were excluded being a rare parameter from analysis but an enhance mechanical system needs to be devised which can control the patching when it is needed to overcome such problems. Table 1singular design change was feasibly good as paralleled to plural alteration. V-grooved shaped riblet of 100µm in height when tested for turbine wing design showed an improvement of 6% alike shape is integrated for our study and found near analogous result .Where it is seen that when add-in is introduced near the tail, decreases the overall pressure directly effecting efficiency. Table 1comparison show wing with add-in (square) better than simple wing with point 0 pressure value of 4300 Pa, 6200 Pa where at point 0.05 it gave 500 Pa, 4000 Pa and at 0.1 it had 100 Pa, 100 Pa. Hence, this shows that additional geometric changes make positive effect in some cases given that they are made on specific location like in front section or rear section. More work needs to be done in respect to study 3D cases of such problems; a practically good solution can lead to better fuel efficiency.

5. REFERENCES

1. Duan, L. & M.M. Choudhari. *Effects of Riblets on Skin Friction in High-Speed Turbulent Boundary Layers*. NASA Langley Research Center, Hampton, VA, USA (2012).

2. Sareen, A., R.W. Deters, S.P. Henry, & M.S. Selig. Drag reduction using riblet film applied to airfoils for wind turbines. *Journal of Solar Energy Engineering* 136(2): 021007-021007-8 (2014).

3. Chamorro, L., R. Arndt, & F. Sotiropoulos. Drag reduction of large wind turbine blades through riblets: Evaluation of riblet geometry and application strategies. *Renewable Energy* 50: 1095-1105 (2013).

4. Li, Y. & J. Wang. Experimental studies on the drag reduction and lift enhancement of a delta wing. *Journal of Aircraft* 40(2): 277-281 (2003).

5. Han, M., H.C.Lim, Y.G. Jang, S.S. Lee, & S.J. June. Fabrication of a micro-riblet film and drag reduction effects on curved objects. In: *12th International Conference on TRANSDUCERS, Solid-State Sensors, Actuators and Microsystems,* , 8-12 June, Boston, USA, 1: 396-399 (2003).

6. Walsh, M.J. Turbulent boundary layer drag reduction using riblets. In: *The American Institute of Aeronautics and Astronautics, Aerospace Sciences Meeting* 1 (1982).

7. Kim, S., J. Kim, J. Park, & J. Choi. Measurements in the wake of an airfoil with regular roughness on the upper surface near the leading edge. *Proceedings of the Institution of Mechanical Engineers, Part G: Journal of Aerospace Engineering* 220(3): 203-208 (2006).

8. Klän, S., S. Burgmann, T. Bachmann, M. Klaas, H. Wagner & W. Schröder. Surface structure and dimensional effects on the aerodynamics of an owl-based wing model. *European Journal of Mechanics - B/Fluids* 33: 58-73 (2012).

9. M. Bartenwerfer & D. Bechert. The viscous flow on hairy surfaces, In: *6th European Drag Reduction Working Meeting, Eindhoven/Nederland,* p. 21–22 (1991).

10. Bechert, D., M. Bruse, W. Hage & R. Meyer. Fluid Mechanics of Biological Surfaces and their Technological Application. *Naturwissenschaften* 87(4): 157-171 (2000).

11. Bixler, G. & B. Bhushan. Bioinspired rice leaf and butterfly wing surface structures combining shark skin and lotus effects. *Soft Matter* 8(44): 11271-11284 (2012).

12. Martin, S. & B. Bhushan. Fluid flow analysis of a shark-inspired microstructure. *Journal of Fluid Mechanics* 756: 5-29 (2014).

13. Konovalov, S., Y. Lashkov & V. Mikhailov. Effect of longitudinal riblets on the aerodynamic characteristics of a straight wing. *Fluid Dynamics* 30(2): 183-187 (1995).

14. Lee, S. & Y. Jang. Control of flow around a NACA 0012 airfoil with a micro-riblet film. *Journal of Fluids and Structures* 20(5): 659-672 (2005).

15. Kairouz, K. & H. Rahai. Turbulent junction flow with an upstream ribbed surface. *International Journal of Heat and Fluid Flow* 26(5): 771-779 (2005).

16. Abbas, A., J. de Vicente & E. Valero. Aerodynamic technologies to improve aircraft performance. *Aerospace Science and Technology* 28(1): 100-132 (2013).

17. Grüneberger, R., F. Kramer, E. Wassen, W. Hage,

R. Meyer & F. Thiele. Influence of wave-like riblets on turbulent friction drag. *Nature-Inspired Fluid Mechanics* 311-329(2012).

18. ANSYS14.5 manual, article 7.1 (2014).

19. Welty, J.R., C.E. Wicks, G. Rorrer & R.E. Wilson. *Fundamentals of Momentum, Heat and Mass Transfer*. John Wiley & Sons, New York (2009).

20. Boiko, A.V., V.V Kozlov, V.V. Syzrantsev & V.A. Shcherbakov. Riblet control of the laminar-turbulent transition in a stationary vortex on an oblique airfoil. *Journal of Applied Mechanics and Technical Physics* 37(1): 69-79 (1996).

21. Saggu, J. & J. Fielding. An integrated CADCAM method for the design and construction of aircraft wing components. *Computers in Industry* 12(2): 123-130(1989).

22. Anon. [Image] Available at: http://www.formula1-dictionary.net/coanda_effect.html (2016) [Accessed 4 Feb. 2016].

23. Xfoil Online Software. BOEING 737 MIDSPAN AIRFOIL - Boeing Commercial Airplane Company model 737 airfoils.Co-efficient of Lift VS Angle of Attack. < http://airfoiltools.com/airfoil/details?airfoil=b737b-il#polars >[Accessed 4 Feb. 2016].